Activating mutations in *STIM1* and *ORAI1* cause overlapping syndromes of tubular myopathy and congenital miosis

Vasyl Nesin[a], Graham Wiley[b], Maria Kousi[c], E-Ching Ong[a], Thomas Lehmann[d], David J. Nicholl[e], Mohnish Suri[f], Nortina Shahrizaila[g], Nicholas Katsanis[c], Patrick M. Gaffney[b], Klaas J. Wierenga[h,1], and Leonidas Tsiokas[a,1]

[a]Department of Cell Biology, University of Oklahoma Health Sciences Center, Oklahoma City, OK 73104; [b]Arthritis and Clinical Immunology Research Program, Oklahoma Medical Research Foundation, Oklahoma City, OK 73104; [c]Center for Human Disease Modeling, Duke University Medical Center, Durham, NC 27710; [d]Department of Hematology, Center for Laboratory Medicine, Kantonsspital St. Gallen, 9001 St. Gallen, Switzerland; [e]Department of Neurology, City Hospital, Birmingham B18 7QH, United Kingdom; [f]Nottingham Clinical Genetics Service, Nottingham University Hospitals National Health Service Trust, City Hospital Campus, Nottingham NG5 1PB, United Kingdom; [g]Division of Neurology, Department of Medicine, Faculty of Medicine, University of Malaya, 50603 Kuala Lumpur, Malaysia; and [h]Section of Genetics, Department of Pediatrics, University of Oklahoma Health Sciences Center, Oklahoma City, OK 73104

Edited by Michael D. Cahalan, University of California, Irvine, CA, and approved February 11, 2014 (received for review July 2, 2013)

Signaling through the store-operated Ca^{2+} release-activated Ca^{2+} (CRAC) channel regulates critical cellular functions, including gene expression, cell growth and differentiation, and Ca^{2+} homeostasis. Loss-of-function mutations in the CRAC channel pore-forming protein ORAI1 or the Ca^{2+} sensing protein stromal interaction molecule 1 (STIM1) result in severe immune dysfunction and nonprogressive myopathy. Here, we identify gain-of-function mutations in the cytoplasmic domain of STIM1 (p.R304W) associated with thrombocytopenia, bleeding diathesis, miosis, and tubular myopathy in patients with Stormorken syndrome, and in ORAI1 (p.P245L), associated with a Stormorken-like syndrome of congenital miosis and tubular aggregate myopathy but without hematological abnormalities. Heterologous expression of STIM1 p.R304W results in constitutive activation of the CRAC channel in vitro, and spontaneous bleeding accompanied by reduced numbers of thrombocytes in zebrafish embryos, recapitulating key aspects of Stormorken syndrome. p.P245L in ORAI1 does not make a constitutively active CRAC channel, but suppresses the slow Ca^{2+}-dependent inactivation of the CRAC channel, thus also functioning as a gain-of-function mutation. These data expand our understanding of the phenotypic spectrum of dysregulated CRAC channel signaling, advance our knowledge of the molecular function of the CRAC channel, and suggest new therapies aiming at attenuating store-operated Ca^{2+} entry in the treatment of patients with Stormorken syndrome and related pathologic conditions.

human genetics | calcium signaling

Ca^{2+} influx in response to the depletion of intracellular Ca^{2+} stores, or store-operated Ca^{2+} entry, constitutes one of the major routes of Ca^{2+} entry in all animal cells (1). Under physiological conditions, Ca^{2+} influx is activated in response to numerous G protein-coupled receptors and receptor tyrosine kinases signaling via inositol-1,4,5-trisphosphate as a second messenger (2). Store-operated Ca^{2+} entry is mediated primarily by the Ca^{2+} release-activated Ca^{2+} (CRAC) channel (3), which consists of the pore-forming subunits ORAI1–3 (or CRAC modulators 1–3) and Ca^{2+} sensors, STIM1 and STIM2 (4–7). STIM proteins reside in the membrane of endoplasmic reticulum (ER), whereas ORAI proteins reside in the plasma membrane. STIM1 is a single transmembrane-spanning protein (8–12) that, in resting cells, exists as a dimer that binds Ca^{2+} through two EF hand-containing domains located in the ER lumen (13). Depletion of Ca^{2+} in the ER induces a series of molecular events in the conformation and localization of STIM1, initiated by the formation of higher-order oligomers, protein unfolding, and accumulation at discrete sites in the cell where the ER membrane is in close proximity to the plasma membrane (11, 13–16). In these sites, STIM1 binds to the cytosolic C and N termini of ORAI1 (17, 18), resulting in channel activation and generation of a highly Ca^{2+}-selective CRAC current, or I_{CRAC} (3, 19, 20). I_{CRAC} is responsible not only for restoring cytosolic and ER Ca^{2+} concentration, thus maintaining the cell in a Ca^{2+} signaling-competent stage (1), but also for many cellular functions such as regulation of gene expression, exocytosis, proliferation, and apoptosis (1).

Consistent with a fundamental role of the CRAC channel in cell signaling, loss-of-function mutations in *STIM1* or *ORAI1* lead to immune deficiency and nonprogressive myopathy (21–23). However, evidence that gain-of-function mutations in *STIM1* and *ORAI1* can affect human health is only recently starting to emerge. It was shown that mutations in the domain of STIM1 that binds Ca^{2+} (EF hand domain) in resting conditions are associated with nonsyndromic myopathy with tubular aggregates (24). Functional studies demonstrated that these mutations cause hyperactivation of the CRAC channel (24). However, it remains unknown whether myopathy with tubular aggregates is caused by the increased activity of the CRAC channel, increased activity of another Ca^{2+} channel using STIM1 as a sensor (25), or a function of STIM1 that is unrelated to Ca^{2+} signaling, as STIM1 can function independently of ORAI1 (26-28).

Stormorken syndrome [Mendelian Inheritance in Man (MIM) 185070] is a rare autosomal-dominant condition with

Significance

Stormorken syndrome is a rare autosomal-dominant genetic condition characterized by congenital miosis, bleeding diathesis, thrombocytopenia, and proximal muscle weakness. Other manifestations include functional or anatomical asplenia, ichthyosis, headaches, and dyslexia. A milder form of Stormorken syndrome is associated with muscle weakness and congenital miosis, but without hematologic abnormalities. Here we identify the gene mutations responsible for these syndromes and show that both conditions are caused by the hyperactivation of the Ca^{2+} release-activated Ca^{2+} (CRAC) channel. These findings contrast the pathologies associated with loss or diminished function of the CRAC channel, provide new molecular insights of the function of the CRAC channel, and suggest new approaches to combat these conditions by blocking CRAC channel activity.

Author contributions: V.N., G.W., M.K., N.K., P.M.G., K.J.W., and L.T. designed research; V.N., G.W., M.K., E.-C.O., P.M.G., K.J.W., and L.T. performed research; T.L., D.J.N., M.S., and N.S. contributed new reagents/analytic tools; V.N., G.W., M.K., E.-C.O., N.K., P.M.G., K.J.W., and L.T. analyzed data; and K.J.W. and L.T. wrote the paper.

The authors declare no conflict of interest.

This article is a PNAS Direct Submission.

[1]To whom correspondence may be addressed. E-mail: klaas-wierenga@ouhsc.edu or leonidas-tsiokas@ouhsc.edu.

This article contains supporting information online at www.pnas.org/lookup/suppl/doi:10.1073/pnas.1312520111/-/DCSupplemental.

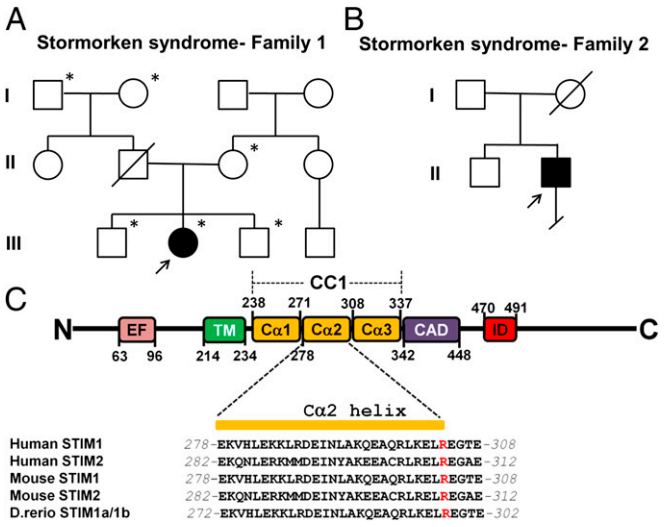

Fig. 1. p.R304W in STIM1 causes Stormorken syndrome. (*A* and *B*) Pedigrees of the two families affected by Stormorken syndrome. Arrows indicate the probands in each family. Asterisk indicates individuals whose whole exome was sequenced. (*C*) Diagram of human STIM1_R304W and sequence alignment of the Cα2 of coiled coil domain 1 (CC1) of WT human, mouse, and zebrafish STIM1 and STIM2. Cα1–3, α-helix 1–3 in CC1; EF, EF hand; ID, inhibitory domain; TM, transmembrane domain.

a constellation of symptoms, including congenital miosis, bleeding diathesis, thrombocytopenia, functional (or anatomical) asplenia, and proximal muscle weakness (29). Other manifestations include ichthyosis, headaches, and dyslexia (30). Patients typically display increased creatine kinase (CK) levels and histologic evidence of myopathy with tubular aggregates (30, 31). Here, we show that Stormorken syndrome is caused by an activating mutation in STIM1. We also identify a mutation in the STIM1-interacting molecule, ORAI1, in a Stormorken-like syndrome that presented with miosis and tubular myopathy. Functional analyses reveal that both mutations enhance the activity of the CRAC channel, but by different molecular mechanisms. These data expand the phenotypic spectrum of activating mutations in the CRAC channels from myopathy with tubular aggregates to miosis, bleeding diathesis, thrombocytopenia, asplenia, ichthyosis, headaches, and dyslexia.

Results

To define the molecular basis of Stormorken syndrome, we performed whole-exome sequencing on the DNA obtained from a child with a symptom complex consistent with Stormorken syndrome (Table S1). We identified a heterozygous frame-shift insertion in Homo sapiens keratin-associated protein 1-1 (*KRTAP1-1*) (NM_030967: c.144_145insGC, p.S48fs) and two heterozygous nonsynonymous mutations, one in RERE arginine-glutamic acid dipeptide (RE) repeats (*RERE*) (NM_012102: c.G4046A, p.R1349Q) and one in *STIM1* (NM_003156: c.910C > T, p.R304W), present only in the proband (patient 1, Table S1). Each of these mutations was validated by Sanger sequencing. Next, we evaluated these mutations by Sanger sequencing in a second, unrelated patient with Stormorken syndrome (patient 2; Fig. 1*B* and Table S1). Although the *KRTAP1-1* and *RERE* mutations were not present in this subject, we confirmed the presence of the identical c.910C>T transition in *STIM1* (Fig. 1*C* and Fig. S1). These results led us to consider the p.R304W in *STIM1* as the molecular lesion in Stormorken syndrome.

The presence of the same mutant allele in two unrelated but phenotypically similar patients argues for a causal role of the p.R304W mutation in Stormorken syndrome. Given the known role of STIM1 in the store-operated Ca^{2+} entry pathway, we measured store-operated Ca^{2+} influx and I_{CRAC} in immortalized lymphocytes derived from our patient with Stormorken syndrome and a healthy individual. Lymphocytes were used instead of platelets for several reasons: (*i*) platelets are not suitable for electrophysiology because of their small size, (*ii*) platelets should have been already preactivated/exhausted, and (*iii*) I_{CRAC} has been extensively studied in B lymphocytes (32) and, therefore, we could test for a direct effect of the Stormorken mutation on native CRAC channel.

Fig. 2*A* shows that lymphocytes derived from the patient with Stormorken syndrome displayed larger Ca^{2+} influx in response to store depletion induced by thapsigargin (TG). Similar results were obtained in primary skin fibroblasts obtained from the same patient (Fig. S2). Next, we recorded native I_{CRAC} in lymphocytes from the Stormorken and healthy individuals. I_{CRAC} was induced by 10mM ethylene glycol tetra-acetic acid (EGTA) added in the recording pipette. Fig. 2 *B* and *C* show constitutive activation of I_{CRAC} and an overall larger size in patient cells compared with normal cells. In addition, fast Ca^{2+}-dependent inactivation (CDI) was suppressed in cells from the patient with Stormorken syndrome (Fig. 2*D*). These data suggested that STIM1_R304W acted as an activating mutation in terms of CRAC channel function.

Next, we sought to investigate the molecular mechanism by which STIM1 p.R304W influences store-operated Ca^{2+} entry through the CRAC channel. To minimize contribution from the WT allele, we used a heterologous system in which HEK293 cells were transfected with STIM1_R304W and ORAI1 and whole-cell currents were measured by using electrophysiology (Fig. 3*A*). Cells transfected with WT STIM1 (STIM1_WT) and ORAI1 were used as controls. In both cases, depletion of intracellular Ca^{2+} stores was induced by 10 mM EGTA added in the recording pipette (Fig. 3*A*). Cells transfected with STIM1_WT showed time-dependent activation and inactivation of I_{CRAC} (Fig. 3*A*, black). Transfection with STIM1_R304W resulted in stable, maximally activated, basal currents (Fig. 3*A*, red),

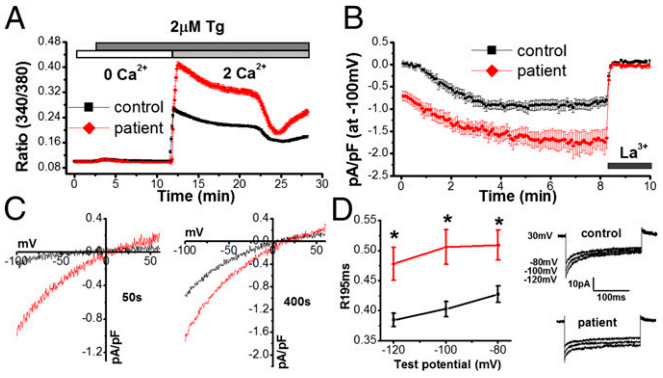

Fig. 2. Store-operated Ca^{2+} entry and I_{CRAC} is enhanced in patients with Stormorken syndrome. (*A*) Store-operated Ca^{2+} entry in lymphocytes obtained from an unaffected individual (control; black, $n = 127$ cells) or a patient with Stormorken syndrome (patient; red, $n = 288$ cells) using single-cell Ca^{2+} imaging. Cells were loaded with 2 μM Fura-2/AM and placed in an extracellular solution (ECS) containing 0 mM Ca^{2+}. Stores were depleted with 2 μM TG and Ca^{2+} influx was stimulated by the addition of 2 mM Ca^{2+} in the ECS. (*B*) Time course of I_{CRAC} in lymphocytes from a control subject (black, $n = 11$ cells) and patient with Stormorken syndrome (red, $n = 16$ cells) induced by 10 mM EGTA in the recording pipette and blocked by 20 μM La^{3+} in the ECS. (*C*) Current–voltage curves taken at 50 s or 400 s after "break-in" in control cells and cells from a patient with Stormorken syndrome. (*D*) Quantification of inactivation as determined by the ratio (R195ms) of the peak current at the beginning of a hyperpolarizing pulse (I_0) to tail current at the end of the pulse (I_{195}) in cells from a healthy individual (black, $n = 11$ cells) and a patient with Stormorken syndrome (red, $n = 16$ cells). Representative step currents generated from hyperpolarizing pulses at the indicated test potentials at 400 s following break-in in a control subject and a patient (Stormorken) cell. Duration of the pulse was 200 ms.

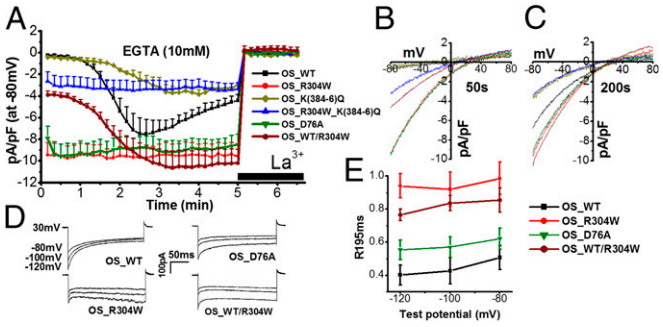

Fig. 3. STIM1_R304W enhances CRAC channel activity in transfected cells. (*A*) Time course of I_{CRAC} in HEK 293 cells transiently cotransfected with ORAI1 plus STIM1_WT (OS_WT; black, $n = 5$), ORAI1 plus STIM1_R304W (OS_R304W; red, $n = 7$), ORAI1 plus STIM1_K(384-6)Q [OS_K(384-6)Q; dark yellow, $n = 5$], ORAI1 plus STIM1_R304W_K(384-6)Q [OS_R304W_K(384-6)Q; blue, $n = 6$], ORAI1 plus STIM1_D76A (OS_D76A; green, $n = 7$), or ORAI1 plus a 1:1 mix of STIM1_WT and STIM1_R304W (OS_WT/R304W; burgundy, $n = 8$) induced by 10 mM EGTA and suppressed by 20 μM La^{3+}. (*B* and *C*) Current–voltage curves taken at 50 (*B*) or 200 s (*C*) after break-in in cells transfected with plasmid combinations shown in *A*. (*D*) Representative step currents generated from hyperpolarizing pulses at the indicated test potentials at 200 s following break-in in cells transfected with OS_WT, OS_R304W, OS_D76A, or OS_WT/R304W in 10 mM extracellular Ca^{2+}. Duration of the pulse was 200 ms. (*E*) Quantification of inactivation as determined by the ratio (R195ms) of the peak current at the beginning of the pulse (I_0) to tail current at the end of the pulse (I_{195}) in cells transfected with OS_WT ($n = 6$), OS_R304W ($n = 7$), D76A ($n = 8$), or OS_WT/R304W ($n = 8$).

displaying the typical current–voltage relationship of I_{CRAC} (Fig. 3 *B* and *C*). The effect of STIM1_R304W on I_{CRAC} was suppressed when STIM1_WT was coexpressed with STIM1_R304W at equal amounts (OS_ST/R304W; Fig. 3*A*, burgundy). The stimulatory effect of STIM1_R304W on I_{CRAC} was also seen when store depletion was induced by 10 mM 1,2-bis(o-aminophenoxy) ethane-N,N,N′,N′-tetraacetic acid (BAPTA), which is a faster Ca^{2+} chelator than EGTA (Fig. S3). In sum, these results showed that, under overexpression conditions, STIM1 p.R304W caused constitutive activation of the CRAC channel. Consistently, STIM1_R304W tagged with YFP at its C terminus (STIM_R304W-YFP) showed a characteristic accumulation in preformed puncta in resting cells, in contrast to STIM1_WT-YFP that showed uniform expression in the ER (Fig. S4).

To obtain further molecular insight of the mechanism by which STIM1_R304W affected I_{CRAC}, we compared and contrasted its function to known loss- and gain-of-function mutant forms of STIM1. STIM1_K(384-6)Q is a triple mutant of STIM1 showing diminished interaction with WT ORAI1 through the CRAC activation domain (CAD) or STIM1 ORAI1 activating region (SOAR) of STIM1 (33). Consistently, transfection of this mutant together with ORAI1 led to slowly activating I_{CRAC} of a significantly smaller size compared with I_{CRAC} induced by STIM1_WT (Fig. 3*A*, dark yellow). Introduction of the R304W mutation to STIM1_K(384-6)Q [STIM1_R304W_K(384-6)Q] led to constitutively active I_{CRAC} but of a size similar to the size of I_{CRAC} induced by STIM1_K(384-6)Q (Fig. 3*A*, blue). These data suggest that STIM1_R304W requires interaction with ORAI1 for the generation of I_{CRAC}. This is consistent with the observation that p.R304W is not located within the CAD/SOAR or within the inhibitory helix (residues 310–340) that binds to and obstructs CAD/SOAR in resting conditions (34). Interestingly, R304 was predicted to make direct contacts with E318 and Q314, both located within an inhibitory helix (35), suggesting that R304W may indirectly affect interactions between the inhibitory helix and CAD/SOAR in resting conditions.

Fig. 3*A* shows that p.R304W causes constitutive activation of the CRAC channel. However, constitutive activation can also occur by mutations in the EF hand of STIM1 (p.H72Q, p.D84G, p.H109R, or p.H109N), identified recently in nonsyndromic forms of tubular-aggregate myopathy (TAM; MIM 160565) (24). These data suggest that, although both types of mutations (in CC1 and EF hand) can be activating, the effect of mutations within CC1 such as p.R304W might be more severe compared with mutations affecting the EF hand. Therefore, we compared directly the effect of STIM1_R304W and STIM1_D76A (36, 37), a well-characterized EF hand mutant, on I_{CRAC}. Although both mutants resulted in constitutively active I_{CRAC} of similar sizes, they differed markedly in the extent of their fast CDI (Fig. 3 *D* and *E*). STIM1_R304W showed no fast CDI, whereas STIM1_D76A showed fast CDI indistinguishable from that of STIM1_WT in 10 mM of extracellular Ca^{2+} (Fig. 3 *D* and *E*). Thus, these results raise the possibility that suppression of the fast CDI could account for the broader phenotypic spectrum of p.R304W in patients with Stormorken syndrome.

To probe further the pathway by which mutations in STIM1 could cause some or all of the pathologic conditions associated with Stormorken syndrome, we searched for mutations associated with Stormorken-like syndromes. In 2004, a Stormorken-like phenotype of proximal muscle weakness and miosis was described in two families, related through distant ancestors (38). Similar to Stormorken syndrome, the muscle weakness in these patients was associated with elevated CK and diagnosed histologically as a myopathy with tubular aggregates (38). However, in contrast to patients with Stormorken syndrome, these individuals lacked evidence of thrombocytopenia, bleeding diathesis, and asplenia (Table S1). Sanger sequencing failed to identify the p.R304W mutation in *STIM1* in two affected siblings from this kindred (Fig. 4*A*). We therefore performed whole-exome sequencing and identified 371 heterozygous variants in 336 genes shared by the two affected siblings. Focusing on genes known to be associated with store-operated Ca^{2+} entry (39), we identified a mutation in *ORAI1* (c.734C>T, p.P245L; Fig. S5), present in both patients. Sanger sequencing in the remaining available members of the family confirmed that the mutation segregated with all seven affected tested but was absent from two unaffected individuals (Fig. 4*A*). P245 is located within the fourth transmembrane helix (M4) of ORAI1 and is conserved from flies to humans (Fig. 4*B*). These results suggest that the p.P245L mutation in *ORAI1* is the molecular cause of this Stormorken-like

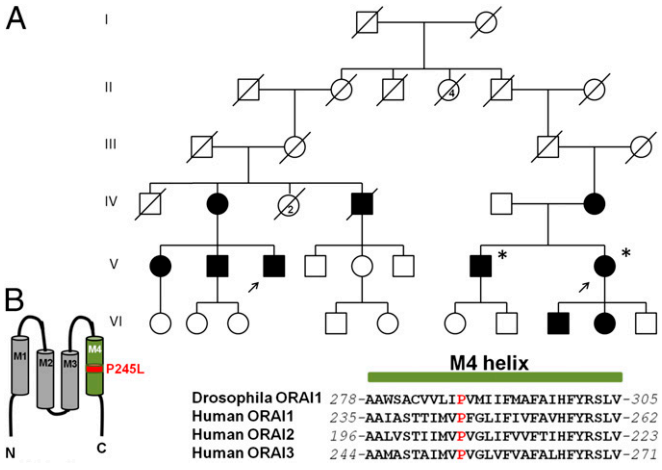

Fig. 4. p.245L in ORAI1 causes a Stormorken-like syndrome with aggregate tubular myopathy. (*A*) Pedigree of the two branches of an extended family with common ancestry in mid-19th century with Stormorken-like syndrome. Branch 1 [Left branch (below generation II)] was described by Shahrizaila et al. (38). The disorder follows an autosomal-dominant inheritance pattern. The arrows indicate the proband in each branch of this family (patient 1, left arrow; patient 2, right arrow). Asterisk indicates individuals whose whole exome was sequenced. (*B*) Cartoon showing the location of P245 in transmembrane segment M4, and a sequence alignment of the M4 α-helix of *Drosophila* ORAI1 and human ORAI1-3.

GENETICS

phenotype in this family and represent, to our knowledge, the first example of a mutation in *ORAI1* associated with a tubular myopathy.

We hypothesized that this mutation may also lead to enhanced CRAC channel activity. To test this hypothesis, we cotransfected STIM1_WT and ORAI1_WT or ORAI1_P245L and measured EGTA-induced I_{CRAC} in HEK293 cells. Fig. 5*A* and Fig. S6 *A* and *B* show that ORAI1_P245L produced I_{CRAC} with similar activation kinetics and peak size, but much reduced inactivation compared with ORAI1_WT. However, fast CDI in ORAI1_P245L was indistinguishable from ORAI1_WT (Fig. S6 *C* and *D*). Induction of I_{CRAC} by 2 mM EGTA (no effect on fast or slow CDI) or 10 mM BAPTA (suppression of fast and slow CDI) in the pipette solution indicated that ORAI1_P245L-transfected cells showed reduced inactivation compared with cells transfected with ORAI1_WT only in cells in which I_{CRAC} was induced by EGTA (Fig. 5 *B* and *C*), indicating that P245L suppressed the slow CDI of ORAI1. These data suggest that, although the CRAC channel was not constitutively active as was seen with STIM1_R304W (Fig. 2*A*) and ORAI1_P245L still required association with STIM1 for activation, ORAI1_P245L-mediated currents showed prolonged activation as a result of reduced slow CDI. To test whether store-operated Ca^{2+} entry was enhanced in cells of a patient with the p.P245L mutation, we measured Ca^{2+} influx in response to store depletion by using TG in immortalized lymphocytes derived from a healthy individual and a patient. As predicted, Ca^{2+} influx developed slower compared with control cells and showed prolonged activation (Fig. 5*D*).

Next, we tested for a possible effect of STIM1_R304W and ORAI1_P245L on hemostasis, one of the features of Stormorken syndrome, in developing zebrafish embryos. Bleeding was visualized directly with o-dianisidine staining of hemoglobin (40) (Fig. 6 *A–G*), whereas thrombocyte (a nucleated cell type equivalent to platelets in zebrafish) numbers were visualized by using the Tg(CD41:GFP) line (Fig. 6 *H–P*). In this line, mature thrombocytes and hematopoietic stem cells/progenitors are labeled by GFP (41). However, thrombocytes can be distinguished from hematopoietic stem cells/progenitors by expressing high levels of GFP (42). We also examined the integrity of the caudal vein in Tg(Fli1:GFP) fish (Fig. S7), in which endothelial cells are marked with GFP (41, 43). We reasoned that reduced thrombocyte activity/numbers might impair the routine surveillance and repair of vessels associated with normal hemostatic function. All three assays yielded the same results. Injection of mouse or human WT or mouse STIM1_K(384-6)Q mRNAs yielded embryos indistinguishable from sham-injected animals in terms of bleeding in the tail or in the cranium (n = 50–100 embryos per experiment, scored blind to injection mixture; Fig. 6*G*), thrombocyte numbers (Fig. 6*P*), and formation of caudal veins. In contrast, STIM1_R304W, STIM1_R304W_K(384-6)Q, or STIM1_D76A mRNA resulted in a severe bleeding phenotype wherein embryos presented with varying degrees of brain hemorrhage and bleeding along the trunk and at the ventral portion of the tail (Fig. 6*G*). The number of cells with high levels of GFP in Tg(CD41:GFP) embryos was also reduced markedly (Fig. 6 *H–P*), and the number of embryos with a hypoplastic caudal vein was increased significantly as well (Fig. S7*E*). In contrast, expression of ORAI1_P245L did not show significant differences in any of the three assays compared with ORAI1_WT (Fig. 6 *G* and *P* and Fig. S7*E*). This is consistent with the lack of hematologic defects in patients carrying the ORAI1_P245L allele. The phenotype and effect of the R304W mutation were specific and consistent with our in vitro model, as injection of blended mixtures of WT and mutant STIM1_R304W attenuated the bleeding phenotype (Fig. 6 *G* and *P* and Fig. S7*E*).

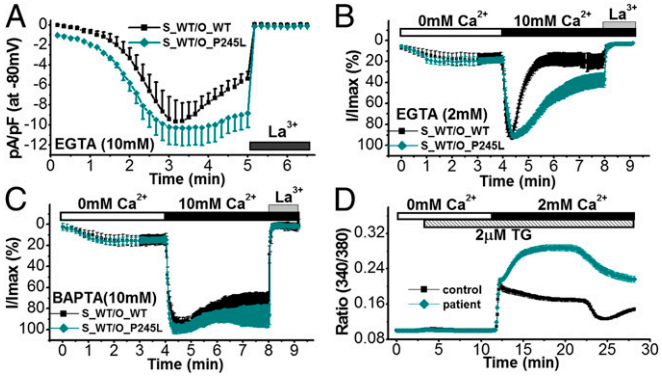

Fig. 5. ORAI1_P245L suppresses slow CDI of I_{CRAC}. (*A*) Time course of I_{CRAC} in HEK293 cells transiently cotransfected with STIM1_WT plus WT ORAI1 (S_WT/O_WT; black, n = 5) or STIM1_WT plus ORAI1_P245L (S_WT/O_P245L; dark cyan, n = 8) induced by 10 mM EGTA and suppressed by 20 μM La^{3+}. (*B*) Normalized whole-cell currents measured at –80 mV of cells transfected with STIM1_WT plus ORAI1_WT (black, n = 10) or STIM1_WT plus ORAI1_P245L (dark cyan, n = 14) in the presence of 2 mM EGTA in the pipette solution. (*C*) Normalized whole-cell currents measured at –80 mV of cells transfected with STIM1_WT plus ORAI1_WT (black, n = 8) or STIM1_WT plus ORAI1_P245L (dark cyan, n = 9) in the presence of 10 mM BAPTA in the pipette solution. (*D*) Store-operated Ca^{2+} entry is enhanced in a patient with congenital miosis and TAM. Store-operated Ca^{2+} entry in lymphocytes obtained from an unaffected individual (control; black, n = 146 cells) or a patient (patient; red, n = 302 cells) using single-cell Ca^{2+} imaging. Cells were loaded with 2 μM Fura-2/AM and placed in an ECS containing 0 mM Ca^{2+}. Stores were depleted with 2 μM TG, and Ca^{2+} influx was stimulated by the addition of 2 mM Ca^{2+} in the ECS.

Discussion

In this study, we show that activating mutations in *STIM1* and *ORAI1*, encoding the primary proteins regulating store-operated Ca^{2+} entry, result in a symptom complex characterized by myopathy with tubular aggregates, congenital miosis and, in the case of *STIM1*, thrombocytopenia and platelet defects. These mutations illustrate the phenotypic effects of hyperactive CRAC channel signaling and contrast the immune deficiency syndrome observed in biallelic loss-of-function mutations in these genes (21–23). Our data are supported by independent studies in mice, in which an activating mutation in the EF hand of STIM1 (p.D84G) led to premature platelet activation and bleeding, one of the symptoms in patients with Stormorken syndrome (44). We note that, in humans, the p.D84G mutation did not have the same effect, raising the possibility that compensatory mechanisms or disease modifiers could account for this difference (24). We propose that, in humans, p.R304W in STIM1 is a stronger activating allele compared with p.P245L in ORAI1 (Table S2). This idea is supported by the more severe effect of p.R304W in STIM1 than that of p.P245L in ORAI1 on I_{CRAC} and bleeding in zebrafish embryos, and thus may explain the broader phenotypic spectrum of patients with Stormorken syndrome. However, p.P245L in ORAI1 appears to be a stronger gain-of-function allele than alleles of STIM1 bearing mutations in the EF hand of STIM1, as EF hand mutants are associated with myopathy without miosis. Our data also suggest that the mechanisms by which STIM1 and ORAI1 function are different in different tissues. It seems that the hemostatic system of platelets is more tolerant to *STIM1/ORAI1* mutations, as thrombocytopenia and bleeding only manifest under conditions in which I_{CRAC} cannot be completely turned off. Partial inactivation of the CRAC channel by preserving fast or slow CDI appears to be tolerated in platelets, as patients with EF hand mutations in *STIM1* or *ORAI1* mutations do not manifest thrombocytopenia or bleeding. However, this is not the case in skeletal muscle cells in which loss of either type of CRAC channel inactivation results in TAM.

Experiments in zebrafish show that overexpression of STIM1_R304W results in thrombocytopenia, bleeding, and hypoplastic caudal vein. Although we are mindful of over fitting human mutational and phenotypic data to a transient in vivo model, our combined data obtained from three separate in vivo assays do suggest that the described phenotypes approximate the Stormorken pathology, certainly within constrains of mechanistic resolution

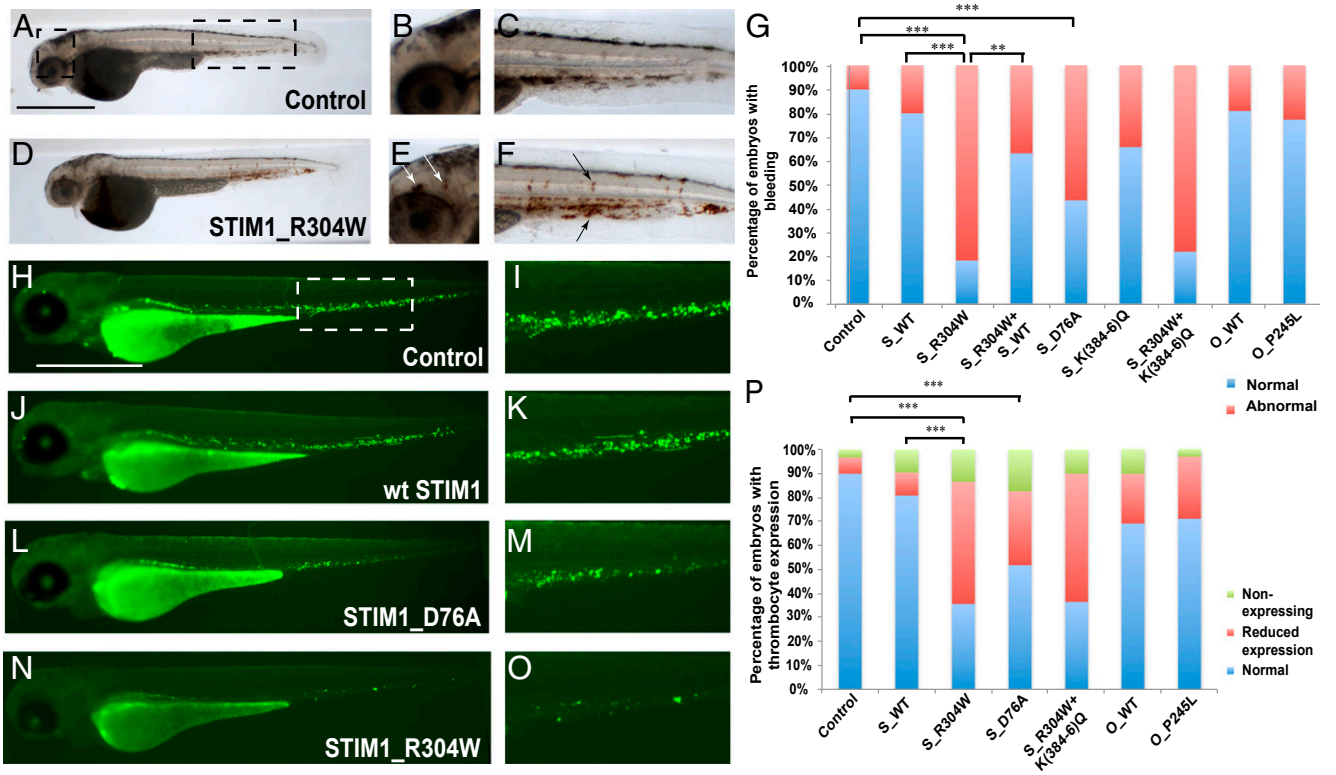

Fig. 6. Expression of STIM1_R304W, but not ORAI1_P245L, results in bleeding and reduced expression and defective flow of thrombocyte progenitors in zebrafish embryos. (*A–F*) Whole-body lateral views of a control (*A*) and STIM1_R304W (*D*) injected embryos at 48 h post fertilization stained with o-dianisidine. *B* and *E* are magnifications of the cephalic boxed area in *A* in all respective embryos, showing brain hemorrhages (white arrows) in the STIM1_R304W mRNA injected embryos (*E*). Panels *C* and *F* show magnified views of the boxed caudal area in *A* in the respective conditions. Areas of intrasomitic and caudal bleeding are highlighted with black arrows. (*G*) Percent distribution of normal embryos vs. embryos with spontaneous bleeding episodes (**$P < 0.001$, ***$P < 0.0001$). (Scale bar: 500 μm.) Whole-body lateral views of control (*H*), STIM1_WT- (*J*), STIM1_D76A- (*L*), and STIM1_R304W- (*N*) injected Tg(CD41:GFP) embryos at 72 h post fertilization. *I*, *K*, *M*, and *O* are magnifications of the ventral boxed area in *H* in the respective embryos, showing expression of GFP in thrombocytes. The boxed area corresponds to the site where early hematopoiesis takes place in zebrafish. (*P*) Percent distribution of normal embryos vs. embryos with reduced or no expression of thrombocyte progenitors (*$P < 0.05$, **$P < 0.001$, and ***$P < 0.0001$).

inherent to this model. All the observed defects are ameliorated when fish are coinjected with the mRNA encoding the WT allele. Although this seems paradoxical, given that patients express an equal amount of WT and mutant alleles, STIM1_R304W is expressed on top of the endogenous WT zebrafish allele. Thus, embryos injected with single mutants also express endogenous WT STIM1. This condition may approximate levels of STIM1_WT and STIM1_R304W in patients with Stormorken syndrome. In addition to recapitulating aspects of Stormorken disease, experiments in zebrafish provided mechanistic insights of the thrombocytopenia induced by STIM1 mutations. Expression of STIM1_R304W_K(384-6)Q resulted in a similar level of bleeding seen with STIM1_R304W (Fig. 6 *G* and *P* and Fig. S7*E*), despite the much larger I_{CRAC} induced by STIM1_R304W (Fig. 3*A*, blue and red). These results suggest that it is the constitutive activation of the CRAC channel, driven by p.R304W, in resting conditions even at a submaximal level, and not necessarily the peak current, that is responsible for the bleeding phenotype in zebrafish embryos. This hypothesis is supported by the lack of an effect of ORAI1_P245L on bleeding and by the suppression of the bleeding phenotype in embryos coinjected with STIM1_R304W and STIM1_WT. This effect could be caused by the reduction of the amount of STIM1_R304W and/or formation of WT/R304W heterodimers, attenuating the constitutive activation of the CRAC channel induced by p.R304W, in resting conditions.

Our study provides molecular insights of the mechanism of CDI of the CRAC channel. We show that not all activating mutations in *STIM1* can have the same effect on the fast CDI of the CRAC channel. For example, the p.R304W mutation residing in the CC1 domain suppressed CDI, which was not seen with the p.D76A mutation residing in the EF hand of STIM1. As fast CDI can be influenced by the ratio of STIM1/ORAI1 proteins in transfected cells (45–47) that could account for the observed differences, it was also shown that STIM1_R304W suppressed, but not abolished, fast CDI in native conditions. These results indicate that there is a role for this residue in modulating fast CDI. However, we do not yet understand how p.R304W suppresses fast CDI, as it is located in a region that is not involved directly in CDI (46).

Our work identifies an activating mutation in ORAI1 associated with a clinical pathologic condition in humans. Functional studies show that the p.P245L in ORAI1 does not cause constitutive activation of the CRAC channel, but rather makes a channel that cannot be completely turned off. In contrast to fast CDI, which is preserved, slow CDI is suppressed by p.P245L. The fact that fast CDI is preserved in ORAI1_P245L is consistent with the mutation being located in a region not involved in the fast CDI (46, 48). Notably, p.P245 in human ORAI1 is equivalent to p.P288 in *Drosophila* ORAI1, the structure of which was recently solved (49). p.P288 was shown to induce a bend in the transmembrane segment M4, suggesting an important structural role of this residue. We speculate that binding of STIM1 to the C-terminal cytosolic domain of ORAI1 induces a structural rearrangement in the transmembrane M4 segment involving P245, which is critical for the slow CDI, perhaps by promoting/stabilizing the STIM1/ORAI1 interaction. Elimination of this bend in the transmembrane M4 segment mediated by the p.P245L mutation could render ORAI1 in a state that stabilizes its interaction with STIM1, making it insensitive to slow CDI. Further work is needed to delineate the

exact molecular mechanisms by which p.P245L in ORAI1 suppresses the slow CDI of the CRAC channel.

Since the first description of tubular aggregates in 1970, evidence has accumulated that these aggregates are inclusions, consisting of regular arrays of tubules derived from the sarcoplasmic reticulum (50). However, the mechanism(s) responsible for the formation of these aggregates is unknown. A relationship between disordered Ca^{2+} metabolism and tubular aggregates has been suggested as early as 1985 (51, 52). We propose that disordered, sustained Ca^{2+} entry through the CRAC channel over long periods of time results in an environment within the sarcoplasmic reticulum that is hostile to protein folding, thus initiating the formation of tubular aggregates. Compounds that target the CRAC channel may be useful therapeutic modalities for alleviating the myopathy and other associated features for patients with these mutations.

Materials and Methods

Patients. The 9-y-old patient with Stormorken syndrome, her two healthy brothers, healthy mother, and two healthy paternal grandparents were enrolled; her father was deceased (Fig. 1*A*). Complete blood count, plasma CK, and platelet aggregation studies were done. A second patient with Stormorken syndrome was recruited to confirm findings (gene/mutation) in our index patient (Fig. 1*B*). Nine individuals from the two branches of the family described by Shahrizaila et al. (38) were recruited, two of whom were phenotypically unaffected (Fig. 4*A*). Genomic DNA was obtained from peripheral blood by using standard protocol from the all individuals mentioned earlier. The study was performed in accordance with the Declaration of Helsinki protocols and was approved by the Oklahoma University Health Sciences Center Institutional Review Board #2866.

Other Materials and Methods. Details on whole exome sequencing, site-directed mutagenesis, Ca^{2+} imaging, electrophysiology, and zebrafish experiments are provided in *SI Materials and Methods*.

Statistical Analysis. Two-tailed *t* tests and χ^2 tests were performed to measure statistical significance between conditions.

ACKNOWLEDGMENTS. We thank all the patients and their families for providing blood and tissue samples; Drs. George Dale, Hongguang Nie, Sanjay Bidichandani, John J. Mulvihill, Mohi Ahmad, and Gerard Elberg for comments on the manuscript; Dr. Richard Marlar and Jana Gausman for performing the platelet aggregation studies; Laura Battiest and Prof. Malcolm Taylor for EBV transformation of B lymphocytes; Drs. Shibo Li and Weihong Xu for skin fibroblast cultures and Sanger sequencing; and Prof. Leonard Zon and Dr. Ilya Shestopalov for providing the Tg(CD41:GFP) zebrafish line. This work was supported by grants from the Oklahoma Center for Adult Stem Cell Research (to L.T.) and the National Institutes of Health (NIH) (R01DK59599 and R01AR64211; to L.T.), and P20GM103456 from the NIH (to P.M.G.), an Oklahoma Medical Research Foundation Institutional Research Grant (to P.M.G.), and R01HD042601 from the NIH (to N.K.).

1. Parekh AB, Putney JW, Jr. (2005) Store-operated calcium channels. *Physiol Rev* 85(2):757–810.
2. Burgess GM, et al. (1984) The second messenger linking receptor activation to internal Ca release in liver. *Nature* 309(5963):63–66.
3. Hoth M, Penner R (1992) Depletion of intracellular calcium stores activates a calcium current in mast cells. *Nature* 355(6358):353–356.
4. Hogan PG, Lewis RS, Rao A (2010) Molecular basis of calcium signaling in lymphocytes: STIM and ORAI. *Annu Rev Immunol* 28:491–533.
5. Soboloff J, Rothberg BS, Madesh M, Gill DL (2012) STIM proteins: Dynamic calcium signal transducers. *Nat Rev Mol Cell Biol* 13(9):549–565.
6. Trebak M (2012) STIM/Orai signalling complexes in vascular smooth muscle. *J Physiol* 590(Pt 17):4201–4208.
7. Vig M, Kinet JP (2009) Calcium signaling in immune cells. *Nat Immunol* 10(1):21–27.
8. Roos J, et al. (2005) STIM1, an essential and conserved component of store-operated Ca2+ channel function. *J Cell Biol* 169(3):435–445.
9. Oritani K, Kincade PW (1996) Identification of stromal cell products that interact with pre-B cells. *J Cell Biol* 134(3):771–782.
10. Liou J, et al. (2005) STIM is a Ca2+ sensor essential for Ca2+-store-depletion-triggered Ca2+ influx. *Curr Biol* 15(13):1235–1241.
11. Zhang SL, et al. (2005) STIM1 is a Ca2+ sensor that activates CRAC channels and migrates from the Ca2+ store to the plasma membrane. *Nature* 437(7060):902–905.
12. Carrasco S, Meyer T (2011) STIM proteins and the endoplasmic reticulum-plasma membrane junctions. *Annu Rev Biochem* 80:973–1000.
13. Liou J, Fivaz M, Inoue T, Meyer T (2007) Live-cell imaging reveals sequential oligomerization and local plasma membrane targeting of stromal interaction molecule 1 after Ca2+ store depletion. *Proc Natl Acad Sci USA* 104(22):9301–9306.
14. Luik RM, Wu MM, Buchanan J, Lewis RS (2006) The elementary unit of store-operated Ca2+ entry: Local activation of CRAC channels by STIM1 at ER-plasma membrane junctions. *J Cell Biol* 174(6):815–825.
15. Wu MM, Buchanan J, Luik RM, Lewis RS (2006) Ca2+ store depletion causes STIM1 to accumulate in ER regions closely associated with the plasma membrane. *J Cell Biol* 174(6):803–813.
16. Lewis RS (2011) Store-operated calcium channels: New perspectives on mechanism and function. *Cold Spring Harb Perspect Biol* 3(12).
17. Park CY, et al. (2009) STIM1 clusters and activates CRAC channels via direct binding of a cytosolic domain to Orai1. *Cell* 136(5):876–890.
18. Yuan JP, et al. (2009) SOAR and the polybasic STIM1 domains gate and regulate Orai channels. *Nat Cell Biol* 11(3):337–343.
19. Penner R, Matthews G, Neher E (1988) Regulation of calcium influx by second messengers in rat mast cells. *Nature* 334(6182):499–504.
20. Lewis RS, Cahalan MD (1989) Mitogen-induced oscillations of cytosolic Ca2+ and transmembrane Ca2+ current in human leukemic T cells. *Cell Regul* 1(1):99–112.
21. Feske S, et al. (2006) A mutation in Orai1 causes immune deficiency by abrogating CRAC channel function. *Nature* 441(7090):179–185.
22. Byun M, et al. (2010) Whole-exome sequencing-based discovery of STIM1 deficiency in a child with fatal classic Kaposi sarcoma. *J Exp Med* 207(11):2307–2312.
23. Picard C, et al. (2009) STIM1 mutation associated with a syndrome of immunodeficiency and autoimmunity. *N Engl J Med* 360(19):1971–1980.
24. Böhm J, et al. (2013) Constitutive activation of the calcium sensor STIM1 causes tubular-aggregate myopathy. *Am J Hum Genet* 92(2):271–278.
25. Zeng W, et al. (2008) STIM1 gates TRPC channels, but not Orai1, by electrostatic interaction. *Mol Cell* 32(3):439–448.
26. Shinde AV, et al. (2013) STIM1 controls endothelial barrier function independently of Orai1 and Ca2+ entry. *Sci Signal* 6(267):ra18.
27. Grigoriev I, et al. (2008) STIM1 is a MT-plus-end-tracking protein involved in remodeling of the ER. *Curr Biol* 18(3):177–182.
28. Smyth JT, Beg AM, Wu S, Putney JW, Jr., Rusan NM (2012) Phosphoregulation of STIM1 leads to exclusion of the endoplasmic reticulum from the mitotic spindle. *Curr Biol* 22(16):1487–1493.
29. Stormorken H, et al. (1985) A new syndrome: thrombocytopathia, muscle fatigue, asplenia, miosis, migraine, dyslexia and ichthyosis. *Clin Genet* 28(5):367–374.
30. Stormorken H (2002) [Stormorken's syndrome]. *Tidsskr Nor Laegeforen* 122(30):2853–2856.
31. Mizobuchi M, et al. (2000) [Muscle involvement of Stormorken's syndrome]. *Rinsho Shinkeigaku* 40(9):915–920.
32. Baba Y, Matsumoto M, Kurosaki T (2013) Calcium signaling in B cells: Regulation of cytosolic Ca(2+) increase and its sensor molecules, STIM1 and STIM2. *Mol Immunol*.
33. Calloway N, Holowka D, Baird B (2010) A basic sequence in STIM1 promotes Ca2+ influx by interacting with the C-terminal acidic coiled coil of Orai1. *Biochemistry* 49(6):1067–1071.
34. Korzeniowski MK, Manjarrés IM, Varnai P, Balla T (2010) Activation of STIM1-Orai1 involves an intramolecular switching mechanism. *Sci Signal* 3(148):ra82.
35. Cui B, et al. (2013) The inhibitory helix controls the intramolecular conformational switching of the C-terminus of STIM1. *PLoS ONE* 8(9):e74735.
36. Navarro-Borelly L, et al. (2008) STIM1-Orai1 interactions and Orai1 conformational changes revealed by live-cell FRET microscopy. *J Physiol* 586(pt 22):5383–5401.
37. Huang GN, et al. (2006) STIM1 carboxyl-terminus activates native SOC, I(crac) and TRPC1 channels. *Nat Cell Biol* 8(9):1003–1010.
38. Shahrizaila N, Lowe J, Wills A (2004) Familial myopathy with tubular aggregates associated with abnormal pupils. *Neurology* 63(6):1111–1113.
39. Fujii Y, et al. (2012) Surf4 modulates STIM1-dependent calcium entry. *Biochem Biophys Res Commun* 422(4):615–620.
40. Albers CA, et al. (2011) Exome sequencing identifies NBEAL2 as the causative gene for gray platelet syndrome. *Nat Genet* 43(8):735–737.
41. Lin HF, et al. (2005) Analysis of thrombocyte development in CD41-GFP transgenic zebrafish. *Blood* 106(12):3803–3810.
42. Ma D, Zhang J, Lin HF, Italiano J, Handin RI (2011) The identification and characterization of zebrafish hematopoietic stem cells. *Blood* 118(2):289–297.
43. Burns CE, et al. (2002) Isolation and characterization of runxa and runxb, zebrafish members of the runt family of transcriptional regulators. *Exp Hematol* 30(12):1381–1389.
44. Grosse J, et al. (2007) An EF hand mutation in Stim1 causes premature platelet activation and bleeding in mice. *J Clin Invest* 117(11):3540–3550.
45. Scrimgeour N, Litjens T, Ma L, Barritt GJ, Rychkov GY (2009) Properties of Orai1 mediated store-operated current depend on the expression levels of STIM1 and Orai1 proteins. *J Physiol* 587(pt 12):2903–2918.
46. Mullins FM, Park CY, Dolmetsch RE, Lewis RS (2009) STIM1 and calmodulin interact with Orai1 to induce Ca2+-dependent inactivation of CRAC channels. *Proc Natl Acad Sci USA* 106(36):15495–15500.
47. Hoover PJ, Lewis RS (2011) Stoichiometric requirements for trapping and gating of Ca2+ release-activated Ca2+ (CRAC) channels by stromal interaction molecule 1 (STIM1). *Proc Natl Acad Sci USA* 108(32):13299–13304.
48. Liu Y, et al. (2012) Crystal structure of calmodulin binding domain of orai1 in complex with Ca2+ calmodulin displays a unique binding mode. *J Biol Chem* 287(51):43030–43041.
49. Hou X, Pedi L, Diver MM, Long SB (2012) Crystal structure of the calcium release-activated calcium channel Orai. *Science* 338(6112):1308–1313.
50. Engel WK, Bishop DW, Cunningham GG (1970) Tubular aggregates in type II muscle fibers: Ultrastructural and histochemical correlation. *J Ultrastruct Res* 31(5-6):507–525.
51. Pierobon-Bormioli S, et al. (1985) Familial neuromuscular disease with tubular aggregates. *Muscle Nerve* 8(4):291–298.
52. Salviati G, et al. (1985) Tubular aggregates: Sarcoplasmic reticulum origin, calcium storage ability, and functional implications. *Muscle Nerve* 8(4):299–306.